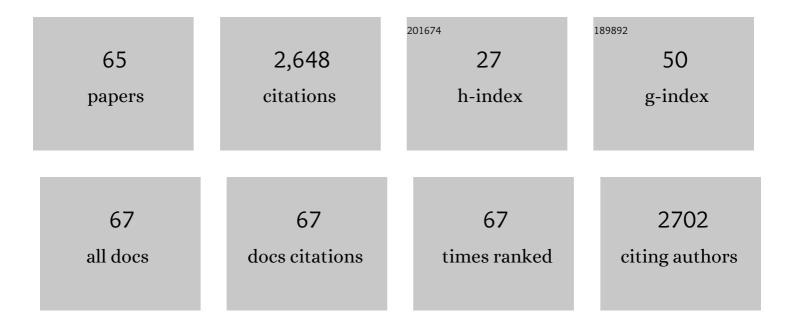
List of Publications by Year in descending order

Source: https://exaly.com/author-pdf/3985365/publications.pdf Version: 2024-02-01



#	Article	IF	CITATIONS
1	Mutual-activation between Zero-Valent iron and graphitic carbon for Cr(VI) Removal: Mechanism and inhibition of inherent Side-reaction. Journal of Colloid and Interface Science, 2022, 608, 588-598.	9.4	15
2	Evaluation of potassium ferrate activated biochar for the simultaneous adsorption of copper and sulfadiazine: Competitive versus synergistic. Journal of Hazardous Materials, 2022, 424, 127435.	12.4	74
3	Effects of pH on light absorption properties of water-soluble organic compounds in particulate matter emitted from typical emission sources. Journal of Hazardous Materials, 2022, 424, 127688.	12.4	10
4	Achieving stably enhanced biological phosphorus removal from aerobic granular sludge system via phosphorus rich liquid extraction during anaerobic period. Bioresource Technology, 2022, 346, 126439.	9.6	13
5	Oxygen doped graphitic carbon nitride with regulatable local electron density and band structure for improved photocatalytic degradation of bisphenol A. Chemical Engineering Journal, 2022, 435, 134835.	12.7	70
6	Evaluation of N-doped carbon for the peroxymonosulfate activation and removal of organic contaminants from livestock wastewater and groundwater. Journal of Materials Chemistry A, 2022, 10, 9171-9183.	10.3	28
7	pH-dependent spectra of particulate water-soluble organic carbon (WSOC) from typical emission sources using EEM-PARAFAC and 2D-COS. Atmospheric Environment, 2022, 287, 119262.	4.1	2
8	The interaction laws of atmospheric heavy metal ions and water-soluble organic compounds in PM2.5 based on the excitation-emission matrix fluorescence spectroscopy. Journal of Hazardous Materials, 2021, 402, 123497.	12.4	22
9	pH-Responsive Fluorescence EEM to Titrate the Interaction between Fluorophores and Acid/Base Groups in Water-Soluble Organic Compounds of PM _{2.5} . Environmental Science and Technology Letters, 2021, 8, 108-113.	8.7	9
10	Heterogeneous activation of peroxymonosulfate for bisphenol A degradation using CoFe2O4 derived by hybrid cobalt-ion hexacyanoferrate nanoparticles. Chemical Engineering Journal, 2021, 404, 127052.	12.7	67
11	Solid-state synthesis of cobalt ferrite fitted with γ-Fe2O3-containing nanocage for peroxymonosulfate activation and cobalt leaching control. Chemical Engineering Journal, 2021, 405, 126994.	12.7	29
12	Local-interaction-field-coupled semiconductor photocatalysis: recent progress and future challenges. Journal of Materials Chemistry A, 2021, 9, 2491-2525.	10.3	48
13	Galvanic corrosion of zero-valent iron to intensify Fe2+ generation for peroxymonosulfate activation. Chemical Engineering Journal, 2021, 417, 128023.	12.7	8
14	Removal of Cd(II) from Micro-Polluted Water by Magnetic Core-Shell Fe3O4@Prussian Blue. Molecules, 2021, 26, 2497.	3.8	14
15	Spectroscopic insight into the pH-dependent interactions between atmospheric heavy metals (Cu and) Tj ETQq1	1 8.78431	14 rgBT /Ove
16	Oxygen vacancies-enriched CoFe2O4 for peroxymonosulfate activation: The reactivity between radical-nonradical coupling way and bisphenol A. Journal of Hazardous Materials, 2021, 418, 126357.	12.4	81
17	Source apportionment of VOCs in a typical medium-sized city in North China Plain and implications on control policy. Journal of Environmental Sciences, 2021, 107, 26-37.	6.1	30
18	Overlooked role of nitrogen dopant in carbon catalysts for peroxymonosulfate activation: Intrinsic defects or extrinsic defects?. Applied Catalysis B: Environmental, 2021, 295, 120291.	20.2	117

#	Article	IF	CITATIONS
19	Modulation of carbon induced persulfate activation by nitrogen dopants: recent advances and perspectives. Journal of Materials Chemistry A, 2021, 9, 25796-25826.	10.3	34
20	Electrochemical recovery of cobalt using nanoparticles film of copper hexacyanoferrates from aqueous solution. Journal of Hazardous Materials, 2020, 384, 121252.	12.4	18
21	Construction of a nanocavity structure with a carrier-selective layer for enhancement of photocatalytic hydrogen production performance. Sustainable Energy and Fuels, 2020, 4, 2164-2173.	4.9	6
22	Synergistic Adsorption and Oxidation of Ciprofloxacin by Biochar Derived from Metal-Enriched Phytoremediation Plants: Experimental and Computational Insights. ACS Applied Materials & Interfaces, 2020, 12, 53788-53798.	8.0	89
23	Electrochemical recovery of low concentrated platinum (Pt) on nickel hexacyanoferrate nanoparticles film. Journal of the Taiwan Institute of Chemical Engineers, 2020, 111, 246-251.	5.3	8
24	Tuning of the Oxygen Species Linker on the Surface of Polymeric Carbon Nitride to Promote the Photocatalytic Hydrogen Evolution Performance. ChemSusChem, 2020, 13, 3605-3613.	6.8	9
25	Tuning of the Oxygen Species Linker on the Surface of Polymeric Carbon Nitride to Promote the Photocatalytic Hydrogen Evolution Performance. ChemSusChem, 2020, 13, 3543-3543.	6.8	1
26	Fluorescence characteristics of particulate water-soluble organic compounds emitted from coal-fired boilers. Atmospheric Environment, 2020, 223, 117297.	4.1	21
27	Attenuation of BPA degradation by SO4â^' in a system of peroxymonosulfate coupled with Mn/Fe MOF-templated catalysts and its synergism with Clâ^' and bicarbonate. Chemical Engineering Journal, 2019, 372, 605-615.	12.7	146
28	Impact of emissions controls on ambient carbonyls during the Asia-Pacific Economic Cooperation summit in Beijing, China. Environmental Science and Pollution Research, 2019, 26, 11875-11887.	5.3	8
29	Preparation, characterization and application in cobalt ion adsorption using nanoparticle films of hybrid copper–nickel hexacyanoferrate. RSC Advances, 2019, 9, 7485-7494.	3.6	10
30	Chemical characteristics of atmospheric carbonyls over the South China Sea: Influence of continental outflow. Atmospheric Environment, 2019, 208, 141-149.	4.1	4
31	Facilitating charge transfer <i>via</i> a giant magnetoresistance effect for high-efficiency photocatalytic hydrogen production. Chemical Communications, 2019, 55, 14478-14481.	4.1	7
32	Synthesis of hybrid-metal hexacyanoferrates nanoparticle films and investigation of its hybrid vigor. Journal of Electroanalytical Chemistry, 2018, 810, 191-198.	3.8	9
33	Well-defined strategy for development of adsorbent using metal organic frameworks (MOF) template for high performance removal of hexavalent chromium. Applied Surface Science, 2018, 457, 1208-1217.	6.1	52
34	Selective removal of cesium by ammonium molybdophosphate – polyacrylonitrile bead and membrane. Journal of Hazardous Materials, 2017, 324, 753-761.	12.4	57
35	Battery-type column for caesium ions separation using electroactive film of copper hexacyanoferrate nanoparticles. Separation and Purification Technology, 2017, 173, 44-48.	7.9	11
36	Rapid Thermal Processing of Microporous Silica Membranes. , 2017, , 317-348.		1

Rapid Thermal Processing of Microporous Silica Membranes. , 2017, , 317-348. 36

#	Article	IF	CITATIONS
37	Allelic diversity in an NLR gene <i>BPH9</i> enables rice to combat planthopper variation. Proceedings of the National Academy of Sciences of the United States of America, 2016, 113, 12850-12855.	7.1	196
38	Cesium adsorption ability and stability of metal hexacyanoferrates irradiated with gamma rays. Journal of Radioanalytical and Nuclear Chemistry, 2015, 303, 1543-1547.	1.5	15
39	Column study on electrochemical separation of cesium ions from wastewater using copper hexacyanoferrate film. Journal of Radioanalytical and Nuclear Chemistry, 2015, 303, 1491-1495.	1.5	21
40	Use low direct current electric field to augment nitrification and structural stability of aerobic granular sludge when treating low COD/NH4-N wastewater. Bioresource Technology, 2014, 171, 139-144.	9.6	37
41	Lead Ions Sorption from Waste Solution Using Aluminum Hydroxide Modified Diatomite. Journal of Environmental Protection, 2014, 05, 509-516.	0.7	6
42	Hexavalent Chromium Removal from Water Using Heat-Acid Activated Red Mud. Open Journal of Applied Sciences, 2014, 04, 275-284.	0.4	23
43	Selective removal of cesium ions from wastewater using copper hexacyanoferrate nanofilms in an electrochemical system. Electrochimica Acta, 2013, 87, 119-125.	5.2	114
44	Thermodynamics and Mechanism Studies on Electrochemical Removal of Cesium Ions from Aqueous Solution Using a Nanoparticle Film of Copper Hexacyanoferrate. ACS Applied Materials & Interfaces, 2013, 5, 12984-12990.	8.0	61
45	A novel tablet porous material developed as adsorbent for phosphate removal and recycling. Journal of Colloid and Interface Science, 2013, 396, 197-204.	9.4	39
46	Removal of Cesium from Aqueous Solutions by Copper Hexacyanoferrate Membrane Coated Electrodes in a Electrochemical Adsorption System. Procedia Engineering, 2012, 44, 1728-1730.	1.2	1
47	Characterization and modification of porous ceramic sorbent for arsenate removal. Colloids and Surfaces A: Physicochemical and Engineering Aspects, 2012, 414, 393-399.	4.7	7
48	Preparation of a film of copper hexacyanoferrate nanoparticles for electrochemical removal of cesium from radioactive wastewater. Electrochemistry Communications, 2012, 25, 23-25.	4.7	54
49	Electrochemical Cesium Recovery Using Nanoparticle Film of Copper Hexacyanoferrate. ECS Meeting Abstracts, 2012, , .	0.0	0
50	Preparation of iron-impregnated tablet ceramic adsorbent for arsenate removal from aqueous solutions. Desalination, 2012, 286, 56-62.	8.2	25
51	Electrochemical Degradation of Chlorsulfuron Herbicide from Water Solution Using Ti/IrO ₂ -Pt Anode. Open Journal of Applied Sciences, 2012, 02, 78-85.	0.4	1
52	How microcystinâ€degrading bacteria express microcystin degradation activity. Lakes and Reservoirs: Research and Management, 2011, 16, 169-178.	0.9	34
53	Development of a ceramic adsorbent for the removal of 2-methylisoborneol from aqueous solution. Desalination, 2011, 281, 293-297.	8.2	1
54	Development of long-life-cycle tablet ceramic adsorbent for geosmin removal from water solution. Applied Surface Science, 2011, 257, 2091-2096.	6.1	12

#	Article	IF	CITATIONS
55	Investigations on the batch and fixed-bed column performance of fluoride adsorption by Kanuma mud. Desalination, 2011, 268, 76-82.	8.2	124
56	Use of ferric-impregnated volcanic ash for arsenate (V) adsorption from contaminated water with various mineralization degrees. Journal of Colloid and Interface Science, 2011, 353, 542-548.	9.4	25
57	Arsenic (V) adsorption on Fe3O4 nanoparticle-coated boron nitride nanotubes. Journal of Colloid and Interface Science, 2011, 359, 261-268.	9.4	135
58	Batch study of arsenate (V) adsorption using Akadama mud: Effect of water mineralization. Applied Surface Science, 2010, 256, 2961-2967.	6.1	27
59	Fluoride removal from water by granular ceramic adsorption. Journal of Colloid and Interface Science, 2010, 348, 579-584.	9.4	120
60	An excellent fluoride sorption behavior of ceramic adsorbent. Journal of Hazardous Materials, 2010, 183, 460-465.	12.4	90
61	Application of simplex-centroid mixture design in developing and optimizing ceramic adsorbent for As(V) removal from water solution. Microporous and Mesoporous Materials, 2010, 131, 115-121.	4.4	37
62	Optimization of process parameters for electrochemical nitrate removal using Box–Behnken design. Electrochimica Acta, 2010, 56, 265-270.	5.2	69
63	Removal of fluoride from aqueous solution by adsorption onto Kanuma mud. Water Science and Technology, 2010, 62, 1888-1897.	2.5	11
64	Application of an electrochemical-ion exchange reactor for ammonia removal. Electrochimica Acta, 2009, 55, 159-164.	5.2	27
65	Simultaneous reduction of nitrate and oxidation of by-products using electrochemical method.	12.4	194